International Journal of Thermodynamics (IJoT)
ISSN 1301-9724 / e-ISSN 2146-1511
https://dergipark.org.tr/en/pub/ijot

Vol. xx (No. x), pp. xxx-xxx, 2025
doi: 10.5541/ijot.1544038
Published online: Mmm dd, 2025

Research Article

Performance Evaluation of Vapor Compression Refrigeration System using CO_2/Propane and CO_2/Propylene Mixtures

* S. Jarungthammachote

Department of Mechanical Engineering, Faculty of Engineering at Sriracha, Kasetsart University, Sriracha, Chonburi, 20230, Thailand
E-mail: *sompop.j@ku.th

Received 5 September 2024, Revised 11 April 2025, Accepted 15 July 2025

Abstract

The search for low GWP refrigerants has become a critical area of research in response to climate change. Natural refrigerants such as carbon dioxide (R744), propane (R290), and propylene (R1270) are particularly promising due to their low GWP. This study theoretically investigates the use of zeotropic mixtures of R744+R290 and R744+R1270 as refrigerants in a vapor compression refrigeration cycle with an internal heat exchanger. A performance analysis of these mixtures was conducted, and the maximum COP and VRC values were investigated according to the compressor discharge pressure (P_H). The effects of ambient air temperature and the mole fraction of R744 on cycle performance were also examined. The results indicate that the R744+R1270 mixture achieves COP and VRC values, on average, 16.5% and 12.2% higher, respectively, than those of the R744+R290 mixture. Furthermore, the optimal compressor discharge pressure for R744+R1270 is, on average, 240 kPa lower than that for R744+R290. When the mole fraction of R744 exceeded 0.6, the lower flammability limit of the mixture increased exponentially. For mole fractions of R744 above 0.36, the maximum COP of the R744+R290 mixture was lower than that of pure R744. An increase in ambient air temperature resulted in a linear rise in the optimal compressor discharge pressure, accompanied by a reduction in both the maximum COP and VRC.

Keywords: *Zeotropic mixtures; CO_2; natural refrigerants; refrigeration system.*

1. Introduction

In recent years, the study of environmentally friendly refrigerants with high coefficients of performance (COP) has become a key focus in refrigeration and air conditioning systems, largely driven by concerns over climate change. Historically, chlorofluorocarbons (CFCs) were widely used as refrigerants. However, these substances were found to severely deplete the ozone layer, leading to the phase-out of both CFCs and hydrochlorofluorocarbons (HCFCs) under the Montreal Protocol [1]. To replace CFCs, hydrofluorocarbons (HFCs) were introduced, offering negligible ozone depletion potential (ODP). However, HFCs possess high global warming potential (GWP) and are now regulated in Europe under the F-gas regulation [2] and the European Parliament's Mobile Air-Conditioning Systems (MAC) Directive No. 40/2006 [3]. Currently, research is focused on the development of fourth-generation refrigerants, as defined by Calm [4], which prioritize zero or very low ODP, low GWP, and high efficiency. The evolution of refrigerants from the 1920s to the 2010s has been thoroughly reviewed by McLinden and Huber [5].

Hydrocarbons (HCs), such as propane (R290) and propylene (R1270), are low-GWP, low-toxicity refrigerants that can be applied in domestic refrigeration systems. These natural refrigerants, however, have high flammability, limiting their widespread application. Corberán et al. [6] reviewed the standards associated with the use of hydrocarbon refrigerants. McLinden et al. [7] studied three refrigeration cycles, a simple vapor compression with and without an internal heat exchanger (IHX) and a two-stage flash economizer cycle, using low-GWP refrigerants, including hydrocarbons. In their analysis, R290 and R170 exhibited superior COPs compared to R410a across all cycles. Kadhim [8] conducted an energy and exergy analysis of a domestic refrigerator using different hydrocarbons as single-component refrigerants. The results showed that at evaporator temperatures of -25°C and -30°C, R1270 had the highest COP, followed by R290. The study recommended using R1270 and R290 as replacements for R134a, combined with a lower displacement compressor and adjustments in the refrigerant charge. Additionally, Bolaji [9] conducted a theoretical investigation of domestic refrigeration systems using mixtures of hydrocarbons (R600a, R600, R290, and R170). The study concluded that these mixtures exhibited significant variations in specific volume, suggesting they could replace R134a with appropriate system modifications.

Carbon dioxide (R744), a natural refrigerant classified in safety group A1 [10], has been used as a refrigerant since the 1920s [4]. Yang et al. [11] noted that R744's energetic efficiency is low under certain operating conditions, but its COP can be improved through two-stage compression with intermediate air supply or by optimizing condensing pressure. A comprehensive review of transcritical R744

*Corresponding Author

cycles in both stationary and transportation refrigeration was provided by Barta et al. [12].

Given that R744 has zero ODP, and is both non-toxic and non-flammable, mixing it with hydrocarbons (HCs) offers a potential solution to mitigate the flammability risks of HCs [13]. Yelishala et al. [14] investigated the performance of a basic vapor compression cycle using pure HCs and R744+HC mixtures, assuming constant heat transfer fluid temperatures at the evaporator and condenser. Their results showed that R744+R1270 exhibited the best performance. A follow-up study by Yelishala et al. [13], incorporating variable heat transfer fluids, found that R744+Dimethyl ether (R-E170) achieved the highest COP, while R744+R1270 had the highest VRC. Sánchez et al. [15] theoretically and experimentally studied binary mixtures of R744 with HFCs and HCs. Their theoretical analysis, focused on improving COP in a single-stage vapor compression cycle with an IHX, showed that the R744+R32 mixture provided the greatest COP improvement at optimal operating conditions. Similarly, Yıldırım et al. [16] investigated the use of R515B as a substitute for R134a in refrigeration systems with IHX, while Direk et al. [17] highlighted the significant performance enhancements possible with IHX. Zhao et al. [18] examined four binary refrigerant mixtures at varying cold space temperatures. Their study found that R744+R1234ze(Z) delivered the highest COP at -45°C, while R744+R600a produced the largest COP at higher temperatures (-35°C and -25°C). This suggests that different refrigerants may be more suitable for specific applications depending on operating conditions.

The literature clearly indicates that hydrocarbons, with their low GWP, are promising refrigerants. Among them, R290 and R1270 demonstrate high performance, but their flammability presents a safety concern. Mixing these hydrocarbons with R744 can reduce the risks associated with accidental leaks. Therefore, the objective of this theoretical study is to investigate the performance of a single-stage vapor compression refrigeration system with an IHX using zeotropic mixtures that are blends of R744+R290 and R744+R1270. The study aims to investigate the performance of these blends as well as determine the optimal compressor discharge pressure for achieving maximum COP. The effects of ambient air temperature and the R744 mole fraction on cycle performance and optimal compressor discharge pressure are also examined.

2. System Configuration and Modeling

2.1 System Description

Figure 1 presents a schematic diagram of the single-stage vapor compression refrigeration system with an internal heat exchanger (IHX) analyzed in this study. The working fluid is a mixture of R744+HC. The cycle starts at point 1, where the low-pressure refrigerant vapor exits the evaporator and enters the compressor. The refrigerant is compressed from state 1 to state 2, raising its pressure and temperature. The high-pressure, high-temperature vapor flows through a condenser or gas cooler (2-3), where it rejects heat to the surrounding air, functioning as the high-temperature reservoir. Depending on the system conditions, the refrigerant may be fully condensed or exist as a supercritical fluid. The condensed refrigerant then transfers energy (3-4) to the lower-temperature refrigerant (6-1) via the IHX. The refrigerant then undergoes an expansion through an expansion valve (4-5), resulting in a reduction in pressure and temperature. The low-pressure, low-temperature refrigerant enters the evaporator, where it absorbs heat from the low-temperature reservoir (5-6). After exiting the evaporator, the refrigerant passes through the IHX, where it gains heat before returning to the compressor inlet, completing the cycle. From state 6 to state 1, the vapor passes back through the IHX, where it is superheated before re-entering the compressor.

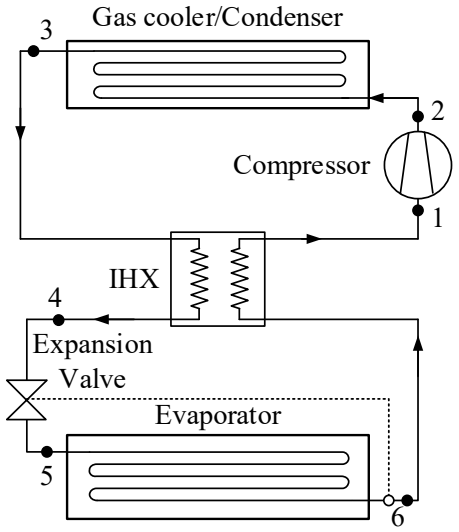

Figure 1. Schematic diagram of the VCRS

2.2 Thermodynamic Modeling

A thermodynamic model of the vapor compression refrigeration system (VCRS) was developed based on the following assumptions.

1. The system operates in a steady-state condition.
2. Pressure drops in the condenser, evaporator, IHX, and connecting tubes are negligible.
3. Heat losses from the compressor and expansion valve are not considered.
4. Refrigerant mixture at the evaporator outlet is a saturated vapor state.
5. The expansion process in the expansion valve is isenthalpic.
6. The isentropic efficiency of the compressor is constant.

The model was implemented in MATLAB, with the thermodynamic properties of all refrigerant mixtures provided by REFPROP v.10 [20]. Figure 2 outlines the calculation procedure for VCRS modeling, while Table 1 lists the input data for the model.

Table 1. Input data to the model

Parameter	Value
Surrounding air temperature (T_{SA})	32°C
Approach temperature in condenser (ΔT_{cond})	4°C
Air inlet temperature at evaporator ($T_{air,in}$)	25°C
Air outlet temperature at evaporator ($T_{air,out}$)	12°C
Effectiveness of IHX (ε_{IHX})	0.7
Isentropic efficiency of compressor (η_C)	0.8
Log. mean temperature difference of evaporator (*LMTD*)	7.0

The model calculation starts with inputting the value of parameters (see Table 1) to the model. The temperature of the refrigerant at the condenser outlet (state 3) relates to the temperature of surrounding air defined by:

$$T_3 = T_{SA} + \Delta T_{cond} \quad (1)$$

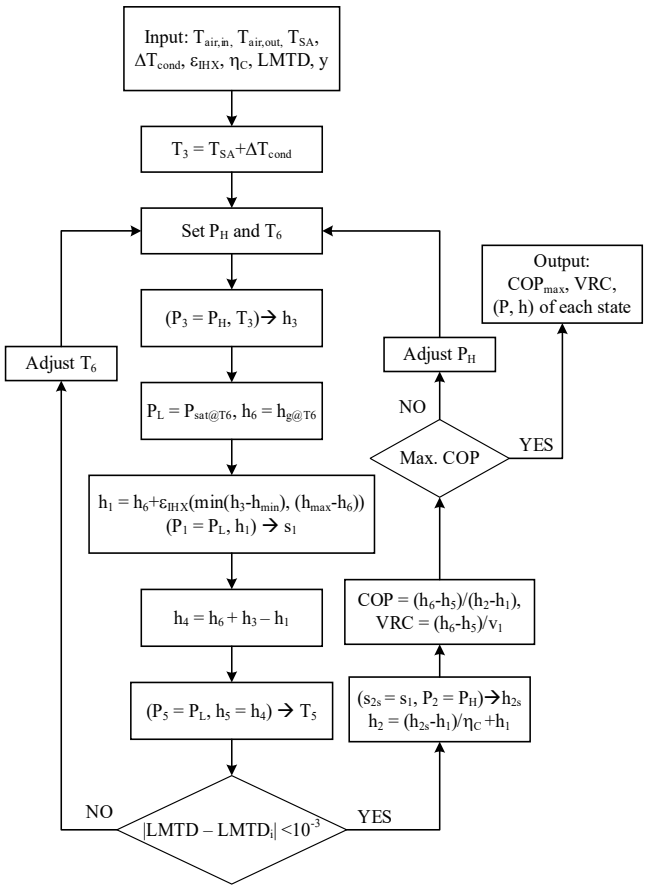

Figure 2. Calculation procedure of the vapor compression refrigeration system.

The high-pressure or the compressor discharge pressure (P_H) and evaporator outlet temperature (T_6) are initially assumed the values. According to assumption 2, it yields $P_2 = P_3 = P_4 = P_H$. Now, state 3 can be defined by P_3 and T_3, allowing the determination of the refrigerant's enthalpy (h_3) as well as other properties at state 3. According to assumption 4, P_6 and h_6 which are a saturation pressure and enthalpy of saturated vapor at T_6, can be obtained. The pressure of states 5 and 1 are also known ($P_5 = P_6 = P_1 = P_L$). State 1 is now defined using P_1 and h_1 which is obtained from the definition of effectiveness of IHX as [19]:

$$\varepsilon_{IHX} = \frac{q_{IHX}}{\min\left[(h_3 - h_{\min}), (h_{\max} - h_6)\right]}, \tag{2}$$

where,

$$q_{IHX} = \left(h_3 - h_4\right) = \left(h_6 - h_1\right) \tag{3}$$

$$h_{\min} = h_4(T = T_6),\ h_{\max} = h_1(T = T_3) \tag{4}$$

where h_{min} is the enthalpy of the refrigerant based on high pressure side and T_6, while h_{max} is the enthalpy of the refrigerant based on low pressure side and T_3. The energy conservation is applied to IHX and the enthalpy of state 4 is obtained as:

$$h_4 = \left(h_6 + h_3 - h_1\right) \tag{5}$$

From assumption 5, $h_5 = h_4$ and $P_5 = P_L$. The temperature at state 5, T_5, can be determined.

The logarithmic mean temperature difference based on the guess value of T_6 can be calculated from

$$LMTD_i = \frac{(T_{air,in} - T_6) - (T_{air,out} - T_5)}{\ln\left(\frac{T_{air,in} - T_6}{T_{air,out} - T_5}\right)} \tag{6}$$

A subscript *i* represents the number of iterations. If the criterion of $|LMTD_i - LMTD| < 10^{-3}$, a calculation of specific compressor work is conducted.

$$w_C = (h_2 - h_1) \tag{7}$$

$$h_2 = h_1 + (h_{2s} - h_1)/\eta_C \tag{8}$$

However, if the criterion is not satisfied, the temperature T_6 is adjusted and the iterative calculation loops continue. Finally, the performance indices, the coefficient of performance (COP) and the volumetric refrigerating capacity (VRC), are evaluated, respectively, by:

$$COP = \frac{q_{evap}}{w_C} = \frac{(h_6 - h_5)}{(h_2 - h_1)} \tag{9}$$

$$VRC = \frac{q_{evap}}{v_1} = \frac{(h_6 - h_5)}{v_1} \tag{10}$$

If the COP is not the maximum, the compressor discharge pressure P_H is adjusted by adding a small pressure of 0.025 MPa to P_H. Iterative calculations are continued until maximum COP is achieved.

In this study, two hydrocarbons, propane (R290) and propylene (R1270), mixed with CO_2 (R744), are investigated. The critical properties and molecular masses of these hydrocarbons and R744 are shown in Table 2 [20]. Table 2 presents the Global Warming Potential (GWP100) [21, 22] and Lower Flammability Limit (LFL) [23] for each refrigerant. The LFL values of the mixtures were calculated based on the extended Le Chatelier's formula, as proposed by Kondo et al. [23]. That is:

$$\frac{c_i}{LFL} = \frac{c_i}{LFL_i} - 0.01094(1 - c) \tag{11}$$

where c_i and LFL_i are the mole fraction and the lower flammability limit, respectively, of R290 or R12870. It is worth noting that the molecular masses of R290 and R744 are nearly identical and higher than that of R1270. However, while the critical pressure and temperature differences between the two hydrocarbons are small, both properties differ obviously from those of R744.

Table 2. Characteristics of refrigerants.

Parameter	R290	R1270	R744
Formula	C_3H_8	C_3H_6	CO_2
M (kg/kmol)	44.0956	42.0797	44.0098
P_c (MPa)	4.2512	4.5550	7.3773
T_c (K)	369.890	364.211	304.128
GWP100	0.02	1.8	1.0

LFL (vol%)	2.03	2.16	-

3. Results and Discussion

3.1 Effect of Compressor Discharge Pressure on Cycle Performance

Figures 3(a) and 3(b) depict the effect of compressor discharge pressure (P_H) on the COP of the cycle using R744+R290 and R744+R1270 mixtures, respectively. The mole fractions used in the simulations are 0.3:0.7 in Figure 3(a) and 0.7:0.3 in Figure 3(b). As shown in Figure 3(a), the COP of both mixtures initially increases with rising P_H. Beyond the point of maximum COP, further increases in P_H lead to a decrease in COP. For R744+R290 mixture, the peak COP occurs at P_H about 3600 kPa, whereas the maximum COP of the cycle using R744+R1270 mixture occurs at P_H about 3450 kPa. The compressor discharge pressure that results in the maximum COP is referred to as the optimal compressor discharge pressure ($P_{H,opt}$). The optimal discharge pressures for both mixtures are lower than their respective critical pressures. While the optimal discharge pressures for the R744+R290 and R744+R1270 mixtures are similar, the maximum COP of the R744+R1270 mixture (4.766) is approximately 0.752 higher than that of the R744+R290 mixture. This indicates an 18.7% increase in COP for the R744+R1270 mixture compared to the R744+R290 mixture. This result shows that R744+R1270 mixture is more interesting than R744+R290 and it indicates the same result from Ref. [8]. Beyond the optimal discharge pressure, increasing the compressor discharge pressure results in a significant decline in COP. Figure 3(b) shows a similar trend, with the maximum COP of the R744+R1270 mixture higher than that of R744+R290, and the optimal pressure for R744+R1270 occurring at a lower discharge pressure. Notably, the maximum COPs for both mixtures with a mole fraction of 0.7:0.3 are on average 5.48% lower than those with a mole fraction of 0.3:0.7.

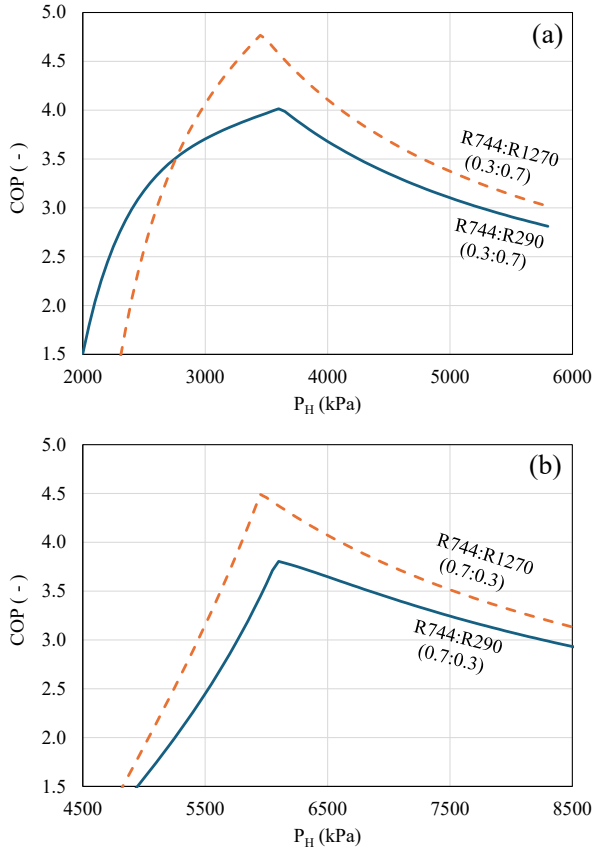

Figure 3. Effect of compressor discharge pressure on COP for refrigerant mixtures with mole fraction of (a) 0.3:0.7 and (b) 0.7:0.3.

Figures 4(a) and 4(b) express the VRCs of different mixtures under varying compressor discharge pressures. For the mole fraction of 0.3:0.7 shown in Figure 4(a) and 0.7:0.3 shown in Figure 4(b), the variation of VRCs in both figures are similar. When the compressor discharge pressure increases, the VRC shapely increases until the optimal compressor discharge pressure is reached, after that further increases in the compressor discharge pressure result in minimal VRC gains.

To further explain the cycle behavior at the optimal and non-optimal discharge pressures, a P-h diagram for the R744+R1270 mixture with a 0.3:0.7 mole fraction is plotted in Figure 5, based on simulation data. It shows that at P_H = 3000 kPa, the cycle cooling capacity is obviously lower than that of the cycle operated at P_H = 3450 and 4000 kPa. This is due to fixed T_3 (indicated by dot-line) and the saturated vapor condition of evaporator outlet. When the compressor discharge

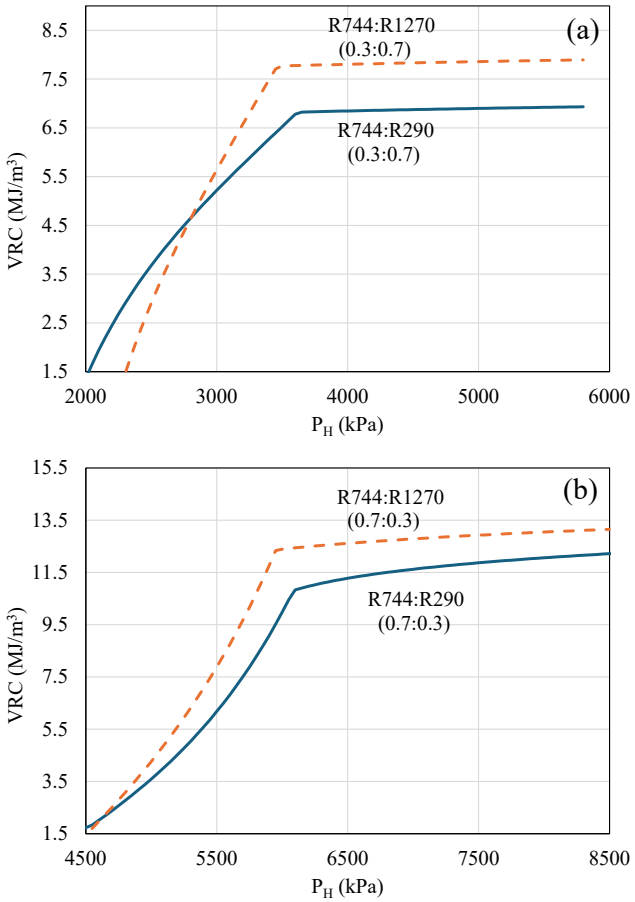

Figure 4. Effect of compressor discharge pressure on VRC for refrigerant mixtures with mole fraction of (a) 0.3:0.7 and (b) 0.7:0.3.

pressure P_H increases util the condenser outlet state becomes a saturated liquid or compressed liquid state, the evaporator inlet state more shift to the left having lower enthalpy. It leads to increasing cooling capacity of the cycle. According to the definition of VCR expressed in Eq. (10) the increase in cooling capacity (numerator) combined with a slight increase in specific volume at the compressor inlet (denominator) leads to a higher VRC.

For COP of the cycle operating at P_H = 3450 kPa compared to that at P_H = 4000 kPa, an increase in the compressor discharge pressure from 3450 kPa to 4000 kPa requires more compression work, while the cooling capacity is almost unchanged (see Figure 5). Therefore, further increase in the compressor discharge pressure above 3450 kPa negatively impacts the cycle's COP.

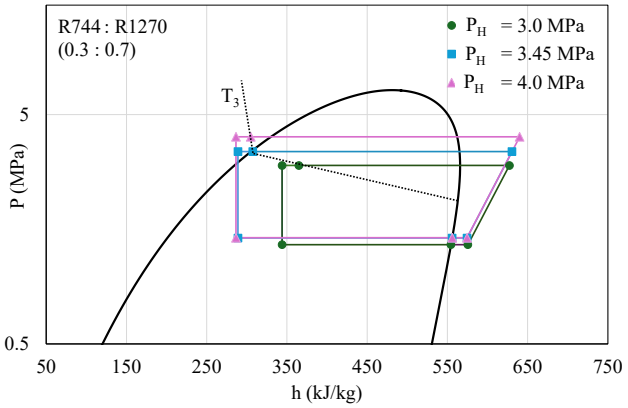

Figure 5. P-h diagram of VRC with IHX using R744+R1270 with mole fraction 0.3:0.7.

3.2 Effect of R744 Concentration

To show the effect of R744 concentration on the performance of the cycle, the mole fraction of R744 in the refrigerant mixtures was varied and COP as well as VRC were investigated. Moreover, other parameters, LFL, the critical pressure and the optimal compressor discharge pressure were also observed.

Figure 6 shows the critical pressure and the optimal compressor discharge pressure for R744+R290 and R744+R1270 blends. The x-axis represents the mole fraction of R744 (ranging from 0.1 to 0.9), while the y-axis indicates pressure in kPa. From the figure, the optimal compressor discharge pressure of R744+R290 and R744+1270 are slightly different when the mole fraction of R744 is less than 0.5. For R744+R290 mixture, the optimal compressor discharge pressure approaches the critical pressure when the mole fraction of R744 equals 0.75, that is 6773 kPa. Beyond this concentration, the cycle becomes a trans-critical cycle to achieve the maximum COP. For R744+R1270 mixture, the optimal compressor discharge pressure remains lower than the critical pressure for mole fractions up to 0.9. When the R744 concentration exceeds 0.9, the optimal discharge pressure surpasses the mixture's critical pressure, and the cycle becomes trans-critical.

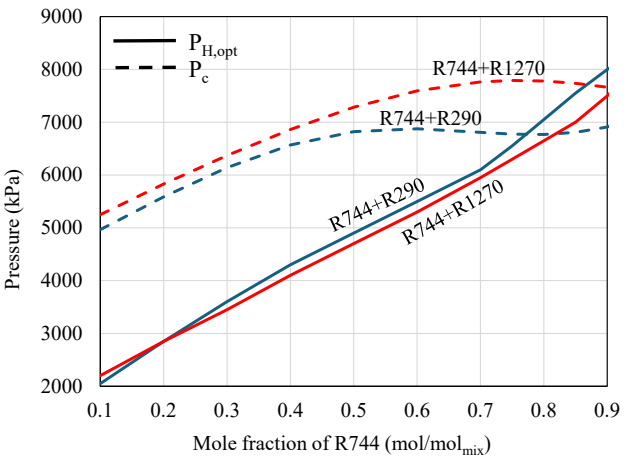

Figure 6. Critical pressure and optimal compressor discharge pressure against mole fraction of R744.

For both mixtures, when the R744 concentration exceeds 0.9, the optimal discharge pressures converge towards 8750 kPa, which is the optimal discharge pressure for pure R744. The critical pressure of R744 in Table 2 indicates that to operate the VCRS using pure R744 following conditions in Table 1, the cycle must run in a trans-critical mode to maximize COP.

Figure 7 shows the effect of R744 concentration on the maximum COP and VRC corresponding to the optimal condition. The VRC of R744+R290 grows from 5.19 to 14.01 MJ/m^3, while that of R744+R1270 rises from 5.95 to 14.27 MJ/m^3. The VRCs of both mixtures almost linearly increase as the mole fraction of R744 increases. However, a slight change in trend occurs when the cycle transitions from sub-critical to trans-critical. It should be noted that the changes in trend of VRC curve and the optimal compressor discharge pressure curve (see Figure 6) coincidently happen.

At a mole fraction of 0.1, the maximum COPs of R744+R290 and R744+R1270 are 5.48 and 5.93, respectively. The maximum COP of both mixtures declines as the R744 concentration increases. For the R744+R290 mixture, the COP begins to rise when the R744 mole fraction reaches 0.5 and then the rate of increase gradually slows. A similar pattern is observed for the R744+R1270 mixture. Overall, the R744+R1270 mixture consistently exhibits a higher COP than the R744+R290 mixture. As illustrated in Figure 7, pure R744 produces a maximum COP of 3.84 (dashed line), while the R744+R1270 mixture outperforms this value across all R744 concentrations. In contrast, the R744+R290 mixture only achieves a higher COP than 3.84 for R744 concentrations between 0.1 and 0.37.

Figure 8 describes the effect of R744 concentration on the value of LFL. LFL of R744+R1270 is on average 7.2% higher than LFL of R744+R290 when compared to LFL of R744+R290. As the mole fraction of R744 increases from 0.1 to 0.6, the LFL of both mixtures increases approximately linearly. However, when the R744 concentration exceeds 0.6, the LFL increases exponentially. At a mole fraction of 0.9, the LFLs of the R744+R290 and R744+R1270 mixtures are 2.536% and 2.778% by volume, respectively. According to the ANSI/ASHRAE Standard 34-2022 [10], both mixtures still fall under Class 3 flammability at this concentration.

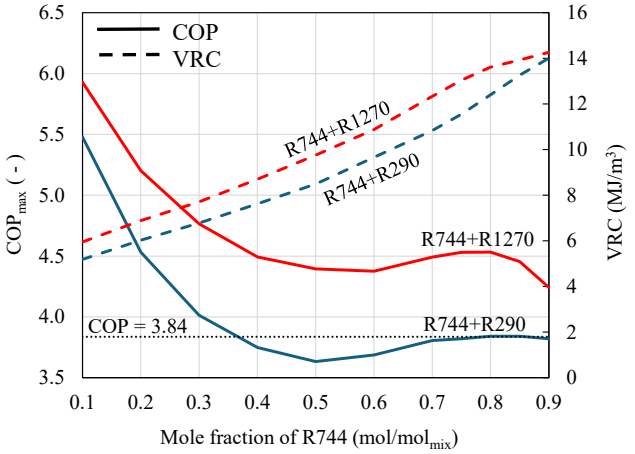

Figure 7. Effect of R744 concentration on the maximum COP and VRC.

However, based on the exponential increase in LFL, it can be inferred that both mixtures will become non-flammable at mole fractions slightly above 0.9. Data from Sánchez et al. [15] indicates that the mass fraction of R744 required to render the mixtures non-flammable is 0.922 for R744+R290 and 0.921 for R744+R1270. Converting from mass fraction to mole fraction may yield slightly different values due to the small differences in molecular masses.

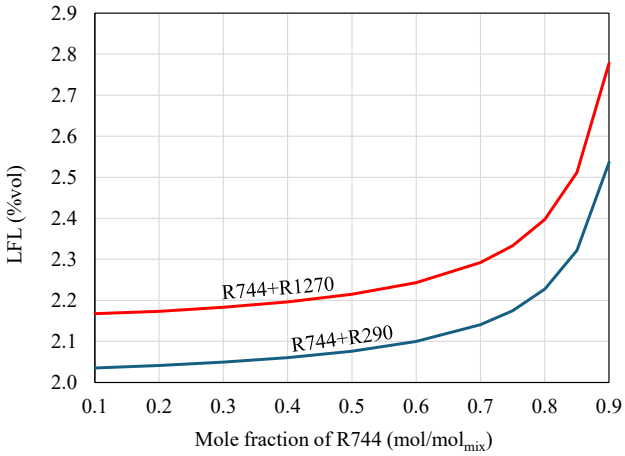

Figure 8. Effect of R744 concentration on LFL of refrigerant.

3.3 Effect of Surrounding Air Temperature

This section explores the effects of surrounding air temperature on the optimal compressor discharge pressure, COP, and VRC. Figure 9 shows how the optimal discharge pressure and COP are affected by the surrounding air temperature. It clearly shows that the optimal compressor discharge pressure of R744+R290 mixture is slightly higher than that of R744+R1270 mixture. As the air temperature rises, the optimal discharge pressures for both mixtures increase linearly. Additionally, the maximum COPs for both mixtures decrease as the surrounding air temperature increases, corresponding to the higher discharge pressures. At optimal discharge pressures, the COP of the R744+R1270 mixture is, on average, 17.2% higher than that of the R744+R290 mixture. However, at higher surrounding air temperature, the different maximum COP of R744+R1270 and R744+R290 slightly increases.

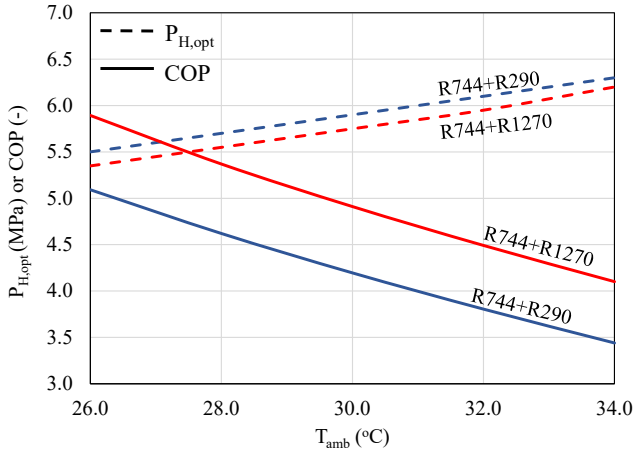

Figure 9. Effect of surrounding air temperature on the optimal compressor discharge pressure and the maximum COP.

The effect of the surrounding air temperature on VRC is also investigated and it is illustrated in Figure 10. The VRC of R744+R1270 is higher than that of R744+R290. The difference of VRC of R744+R1270 and that of R744+R290 expands when the surrounding air temperature increases. This behavior is consistent with the COP trend discussed above. At T_{amb} = 29°C, the VRCs of R744+R1270 and R744+R290 are 13.66 and 12.40 MJ/m^3, respectively. The VRCs of R744+R1270 and R744+R290 reduce to 11.94 and 10.24 MJ/m^3, respectively when T_{amb} = 34°C. It means that, at T_{amb} = 34°C, R744+R1270 mixture can absorb heat 1.7 MJ more than R744+R290 mixture can absorb for the same 1 m^3 of mixture being compressed by compressor.

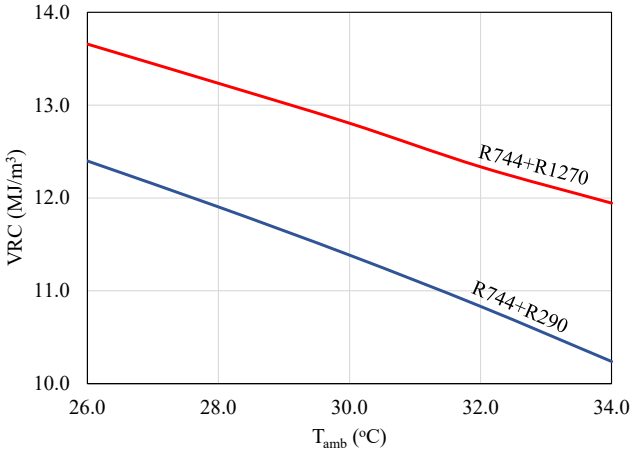

Figure 10. Effect of surrounding air temperature on VRC.

4. Conclusions

This study analyzed the performance of a vapor compression refrigeration system with an internal heat exchanger using CO_2+propane (R744+R290) and CO_2+propylene (R744+R1270) mixtures as refrigerants. The key performance metrics were the coefficient of performance (COP) and volumetric refrigerating capacity (VRC). Special attention was given to determining the optimal compressor discharge pressure that maximizes the COP under specific operating conditions. The effects of various operating parameters on COP and VRC were also examined. The primary conclusions drawn from the study are as follows:

- The optimal compressor discharge pressure for the R744+R1270 mixture is, on average, 240 kPa lower than that for the R744+R290 mixture, even at elevated surrounding air temperatures.
- For mole fractions of R744 between 0.1 and 0.9, the maximum COP of the R744+R1270 mixture is, on average, 16.5% higher than that of the R744+R290 mixture. Additionally, the VRC at maximum COP for the R744+R1270 mixture is, on average, 12.2% greater than that of the R744+R290 mixture.
- The maximum COP of the R744+R1270 mixture can be achieved through subcritical cycle operation when the mole fraction of R744 is between 0.1 and 0.9. In contrast, for the R744+R290 mixture, when the mole fraction of R744 exceeds 0.75, the maximum COP can only be obtained via transcritical cycle operation.
- Increasing the concentration of R744 in the mixtures reduces the maximum COP. However, in the case of the R744+R1270 mixture, the maximum COP is higher than 3.84 which is the COP of pure R744. Moreover, for both R744+R1270 and R744+R290 mixtures, increasing the mole fraction of R744 beyond 0.6 causes an exponential increase in the lower flammability limit (LFL).

- An increase in surrounding air temperature by 2°C results in an 8.7% decrease in the maximum COP for the R744+R1270 mixture, and a 9.3% decrease for the R744+R290 mixture.

Considering the performance results and safety aspects, the R744+R1270 mixture appears more suitable for small to medium-sized domestic cooling systems compared to the R744+R290 mixture.

Nomenclature

COP	*Coefficient of performance*
c	*Mole fraction*
GWP	*Global warming potential*
h	*Specific enthalpy, [kJ/kg]*
IHX	*Internal heat exchanger*
LFL	*Lower flammability limit, [vol %]*
LMTD	*Logarithmic mean temperature difference, [^oC]*
log	*Logaritmic*
M	*Molecular mass, [kg/kmol]*
P	*Pressure, [kPa]*
q	*Specific heat transfer rate, [kJ/kg]*
s	*Specific entropy, [kJ/kg·K]*
T	*Temperature, [^oC]*
VRC	*Volumetric refrigerating capacity, [MJ/m^3]*
w	*Specific work, [kJ/kg]*

Greek Letters

ε	*Effectiveness of heat exchanger*
η	*Isentropic efficiency*

Subscripts

1, 2, …	*State number*
c	*Compressor*
cond	*Condenser*
evap	*Evaporator*
H	*High*
i	*Refrigerant (R290 or R1270)*
in	*Inlet*
L	*Low*
max	*Maximum*
opt	*Optimal value*
out	*Outlet*
SA	*Surrounding air*

Conflict of Interest

The author affirms that, to the best of their knowledge, there is no conflict of interest or common interest with any institution, organization, or individual that may influence the review process of the paper.

References:

[1] United Nations Environment Programme, "The Montreal Protocol on substances that deplete the ozone layer," 2016. Accessed: Jun. 15, 2024. [Online]. Available: https://ozone.unep.org/system/files/documents/MOP-28-12E.pdf.

[2] D. Sánchez, A. Andreu-Nácher, D. Calleja-Anta, R. Llopis and R. Cabello, "Energy impact evaluation of different low-GWP alternatives to replace R134a in a beverage cooler. Experimental analysis and optimization for the pure refrigerants R152a, R1234yf, R290, R1270, R600a and R744," *Energy Convers. Manag.*, vol. 256, Mar. 2022, Art. no. 115388, doi: 10.1016/j.enconman.2022.115388.

[3] Directive 2006/40/EC of the European Parliament and the Council of 17 May 2006 relating to emissions from air-conditioning systems in motor vehicles and amending Council Directive 70/156/EEC, The European Parliament and the Council. [Online]. Available: https://eur-lex.europa.eu/LexUriServ/LexUriServ.do?uri=OJ:L:2006:161:0012:0018:en:PDF.

[4] J. M. Calm, "The next generation of refrigerants – Historical review, considerations, and outlook," *Int. J. of Refrig.*, vol. 31, pp. 1123-1133, Nov. 2008, doi: 10.1016/j.ijrefrig.2008.01.013.

[5] M. O. McLinden and M. L. Huber, "(R)Evolution of Refrigerants," *J. Chem. Eng. Data*, vol. 65, no. 9, pp. 4176-4193, Jul. 2020, doi: 10.1021/acs.jced.0c00338.

[6] J. M. Corberán, J. Segurado, D. Colbourne and J. Gonzálvez, "Review of standards for the use of hydrocarbon refrigerants in A/C, heat pump and refrigeration equipment," *Int. J. Refrig.*, vol. 31, no. 4, pp. 748-756, Jun. 2008, doi: 10.1016/j.ijrefrig.2007.12.007.

[7] M. O. McLinden, J. S. Brown, R. Brignoli, A. F. Kazakov and P. A. Domanski, "Limited options for low-global-warming-potential refrigerants," *Nature Commun.*, vol. 8, no. 1, Feb. 2017, Art. no. 14476, doi: 10.1038/ncomms14476.

[8] S. Ali Kadhim, "Thermodynamic and Environmental Analysis of Hydrocarbon Refrigerants as Alternatives to R134a in Domestic Refrigerator," *Int. J. Thermodyn.*, vol. 27, no. 2, pp. 10-18, Jun. 2024, doi: 10.5541/ijot.1368985.

[9] B. O. Bolaji, "Theoretical assessment of new low global warming potential refrigerant mixtures as eco-friendly alternatives in domestic refrigeration systems," *Sci. Afr.*, vol. 10, Nov. 2020, Art. no. e00632, doi: 10.1016/j.sciaf.2020.e00632.

[10] *Designation and Safety Classification of Refrigerants*, ANSI/ASHRAE Standard 34-2022, ASHRAE, Georgia, USA, 2022.

[11] Z. Yang, B. Feng, H. Ma, L. Zhang, C. Duan, B. Liu, Y. Zhang, S. Chen and Z. Yang, "Analysis of lower GWP and flammable alternative refrigerants," *Int. J. of Refrig.*, vol. 126, pp. 12-22, Jun. 2021, doi: 10.1016/j.ijrefrig.2021.01.022.

[12] R. B. Barta, E. A. Groll and D. Ziviani, "Review of stationary and transport CO_2 refrigeration and air conditioning technologies," *Appl. Therm. Eng.*, vol. 185, Feb. 2021, Art. no. 116422, doi: 10.1016/j.applthermaleng.2020.116422.

[13] S. C. Yelishala, K. Kannaiyan, R. Sadr, Z. Wang, Y. A. Levendis and H. Metghalchi, "Performance maximization by temperature glide matching in energy exchangers of cooling systems operating with natural hydrocarbon/CO_2 refrigerants," *Int. J. of Refrig.*, vol. 119, pp. 294-304, Nov. 2020, doi: 10.1016/j.ijrefrig.2020.08.006.

[14] S. C. Yelishala, K. Kannaiyan, Z. Wang, H. Metghalchi, Y. A. Levendis and R. Sadr, "Thermodynamic Study on

Blends of Hydrocarbons and Carbon Dioxide as Zeotropic Refrigerants," *J. Energy Resour. Technol.*, vol. 142, no. 8, Aug. 2020, Art. no. 082304-1-10, doi: 10.1115/1.4045930.

[15] D. Sánchez, F. Vidan-Falomir, L. Nebot-Andrés, R. Llopis and R. Cabello, "Alternative blends of CO_2 for transcritical refrigeration systems. Experimental approach and energy analysis," *Energy Convers. Manag.*, vol. 279, Mar. 2023, Art. no. 116690, doi: 10.1016/j.enconman.2023.116690.

[16] R. Yıldırım, A. Şencan Şahin and E. Dikmen, "Comparative Energetic, Exergetic, Environmental and Enviroeconomic Analysis of Vapour Compression Refrigeration Systems Using R515B as Substitute for R134a," *Int. J. Thermodyn.*, vol. 25, no. 1, pp. 125-133, Mar. 2020, doi:10.5541/ijot.1011622.

[17] M. Direk, M. S. Mert, F. Yüksel and A. Keleşoğlu, "Exergetic Investigation of a R1234yf Automotive Air Conditioning System with Internal Heat Exchanger," *Int. J. Thermodyn.*, vol. 21, no. 12, pp. 103-109, May 2018, doi: 10.5541/ijot.357232.

[18] Z. Zhao, J. Luo, Q. Song, K. Yang, Q. Wang and G. Chen, "Theoretical investigation and comparative analysis of the Linde–Hampson refrigeration system using eco-friendly zeotropic refrigerants based on R744/R1234ze(Z) for freezing process applications," *Int. J. of Refrig.*, vol. 145, pp. 30-39, Jan. 2023, doi: 10.1016/j.ijrefrig.2022.09.036.

[19] R. A. Otón-Martínez, F. Illán-Gómez, J. R. García-Cascales, F. Velasco and M. Reda Haddouche, "Impact of an internal heat exchanger on a transcritical CO_2 heat pump under optimal pressure conditions: Optimal-pressure performance of CO_2 heat pump with IHX," *Appl. Therm. Eng.*, vol. 215, Art. no. 118991, Oct. 2022, doi: 10.1016/j.applthermaleng.2022.118991.

[20] M. L. Huber, E. W. Lemmon, I.H. Bell, M. O. McLinden, "The NIST REFPROP Database for Highly Accurate Properties of Industrially Important Fluids," *Industrial & Engineering Chemistry Research*, vol.61, no. 42, pp. 15449-15472, Jun. 2022, doi: 10.1021/acs.iecr.2c01427.

[21] Intergovernmental Panel on Climate Change, Climate Change 2007: The Physical Science Basis. Cambridge, UK: Cambridge University Press, 2007.

[22] Intergovernmental Panel on Climate Change, Climate Change 2021: The Physical Science Basis, Cambridge, UK: Cambridge University Press, 2021.

[23] S. Kondo, K. Takizawa, A. Takahashi and K. Tokuhashi, "Extended Le Chatelier's formula for carbon dioxide dilution effect on flammability limits," *J. Hazard. Mater.*, vol. 138, pp. 1-8, Nov. 2006, doi: 10.1016/j.jhazmat.2006.05.035.